

**Transport of Water to the Martian Upper Atmosphere amid Regional and Global Dust Storms.** S. W. Stone,<sup>1</sup> R. V. Yelle,<sup>1</sup> M. Benna,<sup>2</sup> M. K. Elrod,<sup>2</sup> and P. R. Mahaffy,<sup>3</sup> <sup>1</sup>Lunar and Planetary Laboratory, University of Arizona (stone@lpl.arizona.edu), <sup>2</sup>Planetary Environments Laboratory, NASA Goddard Space Flight Center, <sup>3</sup>Solar System Exploration Division, Code 690, NASA Goddard Space Flight Center.

**Introduction:** Though Mars is currently cold and dry, it was warmer and wetter billions of years ago. Enrichment of D/H in the Martian atmosphere and surface minerals relative to that of Earth indicates that the vast majority of Mars' water was lost to space over the last ~4 billion years.[1] Water in the lower atmosphere cannot diffuse upward beyond the hygropause, but H<sub>2</sub> produced by the photodissociation of H<sub>2</sub>O and the odd hydrogen (HO<sub>x</sub>) cycle can diffuse into the upper atmosphere. There, H<sub>2</sub> is destroyed by ion-neutral reactions and photodissociation, producing H which escapes to space.[2,3] The H<sub>2</sub> that penetrates into the exosphere can also escape, though there exists only one measurement of the H<sub>2</sub> abundance in the Martian upper atmosphere. Thus, constraints on H<sub>2</sub> loss are relatively poor and modeled H<sub>2</sub> escape fluxes vary widely.[4-7] The NASA Mars Atmosphere and Volatile Evolution (MAVEN) Neutral Gas and Ion Mass Spectrometer (NGIMS) collects *in situ* measurements of neutral and ionic abundances in the Martian upper atmosphere. Using NGIMS measurements of water-related ions (e.g. H<sub>2</sub>O<sup>+</sup> and H<sub>3</sub>O<sup>+</sup>) obtained during a localized dust storm in Mars year (MY) 32 and the global dust storm of MY 34, we demonstrate the effects of rapid and direct delivery of water, another source of H, to the upper atmosphere of Mars, which could result in acute acceleration of H escape. We carry out calculations to obtain H<sub>2</sub>O and H<sub>2</sub> abundances in this region and investigate the variation of these sources of hydrogen during these dust events.

Slow and steady delivery of H<sub>2</sub> from the lower atmosphere cannot explain recent observations of rapid order-of-magnitude variations in the exospheric H abundance and escape flux.[8-11] These variations correlate with Martian season and dust activity in the lower atmosphere, peaking in southern summer when Mars is closest to the Sun. The most likely cause for rapid variation in the exospheric H abundance is direct transport of water — the most abundant hydrogen-bearing species in the Martian atmosphere — into the middle and upper atmosphere.[12-14] This transport is possible due to a weakening of the hygropause, which is warmed and raised in altitude as a result of heating caused by atmospheric dust and increased solar insolation around perihelion. Once in the upper atmosphere, H<sub>2</sub>O is destroyed, forming H.

There is strong circumstantial evidence connecting dust activity in the lower atmosphere and direct transport of water into the middle and upper

atmosphere to observed rapid increases in the H escape rate at Mars, but until now there has been no direct evidence for the presence and effects of this water in the upper atmosphere. We unambiguously detect the chemical intermediates that lie between water delivered from the lower atmosphere and H escape from the top of the atmosphere using direct measurements of ions produced through ionization and dissociation of water. Assuming photochemical equilibrium, H<sub>2</sub>O and H<sub>2</sub> abundances are calculated, providing insight into the upward transport and variation in the upper atmosphere of these hydrogen reservoirs, with a particular focus on localized dust activity during MY 32 and the global dust storm of MY 34. Calculated H production rates demonstrate that H<sub>2</sub>O can become a significant source of escaping H during these events.

**Variation of Protonated Ions During Dust Storms:** The abundances of water-related ions H<sub>2</sub>O<sup>+</sup> and H<sub>3</sub>O<sup>+</sup> increase markedly in the lower thermosphere after the onset of dust activity during a local dust storm in MY 32 and the planet-encircling dust storm of MY 34 (**Figure 1**). These two species are produced mainly by charge transfer from CO<sub>2</sub><sup>+</sup> to H<sub>2</sub>O (to give H<sub>2</sub>O<sup>+</sup>) and proton transfer from HCO<sup>+</sup> to H<sub>2</sub>O (to give H<sub>3</sub>O<sup>+</sup>).[3] During the regional dust storm of MY 32, the mean H<sub>2</sub>O<sup>+</sup> abundance at periapsis (a CO<sub>2</sub> density of 10<sup>9</sup> cm<sup>-3</sup>) increases by a factor of 2 from 1.55 to 3.14 cm<sup>-3</sup>, and the mean periapsis H<sub>3</sub>O<sup>+</sup> abundance increases by a factor of 1.4, from 0.110 to 0.153 cm<sup>-3</sup>. As can be

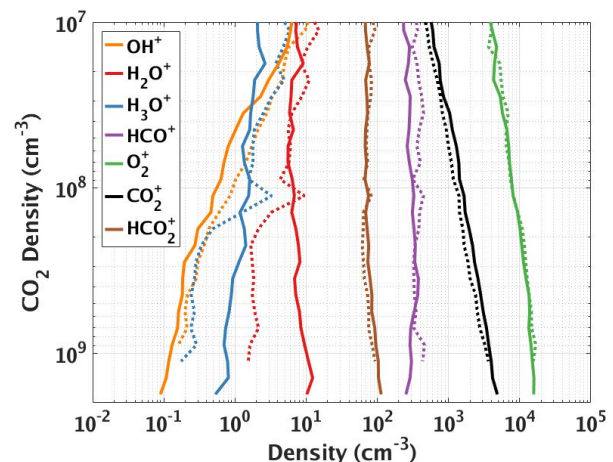


**Figure 1.** Mean ion abundance profiles measured by MAVEN NGIMS before (dotted) and during (solid) the MY 34 global dust storm.

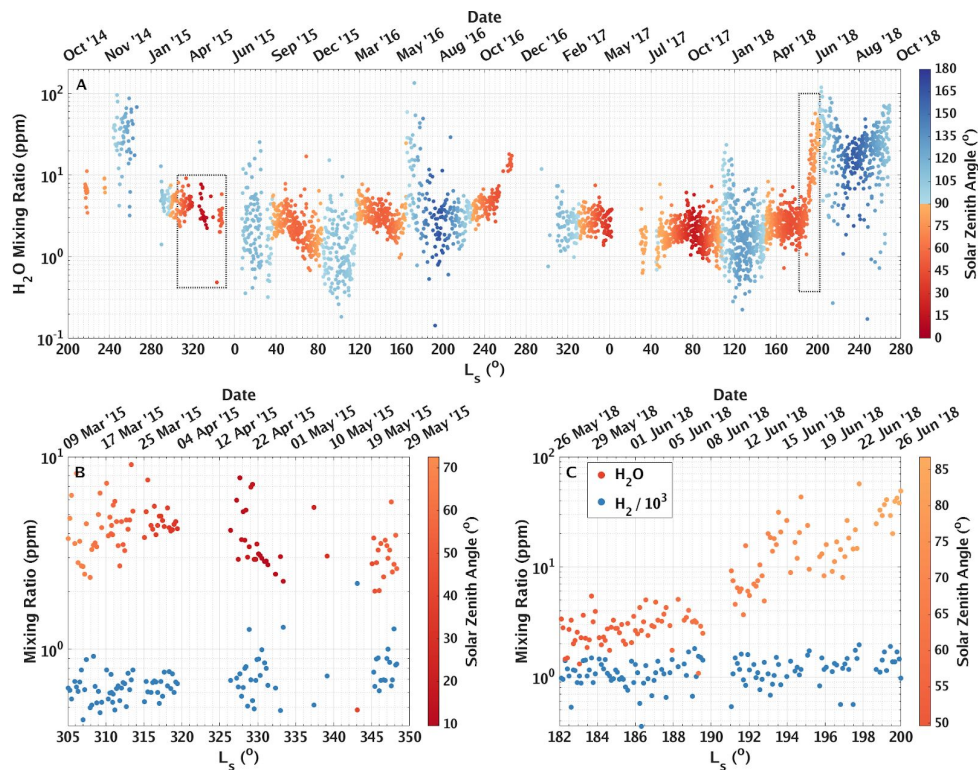


**Figure 2.** Mean H<sub>2</sub>O mixing ratios for each MAVEN orbit (A) over the course of the mission thus far, (B) during a local dust storm in MY 32, and (C) during the MY 34 global dust storm. Each point represents the mean H<sub>2</sub>O (color according to colorbar) or H<sub>2</sub> (dark blue) mixing ratio between CO<sub>2</sub> densities of  $5 \times 10^8$  and  $10^9$  cm<sup>-3</sup> for a single orbit.

seen in **Figure 1**, the mean periaresis H<sub>2</sub>O<sup>+</sup> abundance increases by more than a factor of 6, from 1.58 to 10.1 cm<sup>-3</sup> during the MY 34 global dust storm and the mean periaresis H<sub>3</sub>O<sup>+</sup> abundance increases by more than a factor of 3, from 0.235 to 0.742 cm<sup>-3</sup>.

**Delivery of Water to the Upper Atmosphere:** Theorizing that the increases in H<sub>2</sub>O<sup>+</sup> and H<sub>3</sub>O<sup>+</sup> are due to an influx of H<sub>2</sub>O in the upper atmosphere, we calculate H<sub>2</sub>O abundances, assuming photochemical equilibrium, from NGIMS H<sub>2</sub>O<sup>+</sup>, H<sub>3</sub>O<sup>+</sup>, and HCO<sup>+</sup> measurements. The variation of the H<sub>2</sub>O mixing ratio over the course of the MAVEN mission is shown in **Figure 2**. The calculations demonstrate a significant injection of water into the lower thermosphere during these events. In MY 32, between CO<sub>2</sub> densities of  $5 \times 10^8$  and  $10^9$  cm<sup>-3</sup>, the H<sub>2</sub>O mixing ratio increases by 10%, from 4.55 to 4.88 ppm. In MY 34, the water abundance increased by a factor of 2.4 from a mean value of 2.97 ppm prior to the onset of the global dust storm to 7.07 ppm after the onset of storm. Each of these values is the mean H<sub>2</sub>O mixing ratio over 10 orbits prior to and during each dust storm.

**Molecular Hydrogen in the Upper Atmosphere:** To investigate the potential contribution of H<sub>2</sub> to variations in the abundances of

protonated ions, H<sub>2</sub> abundances were calculated from NGIMS ion measurements. The H<sub>2</sub> abundance is relevant as H<sub>2</sub> can escape from the Martian atmosphere and reacts with numerous ions (mainly CO<sub>2</sub><sup>+</sup>) to produce H, which can also escape. In **Figure 2**, the mean H<sub>2</sub> mixing ratio between CO<sub>2</sub> densities of  $5 \times 10^8$  and  $10^9$  cm<sup>-3</sup> is shown in panels **B** and **C**. The H<sub>2</sub> mixing ratio does not change significantly during the two dust events discussed herein.

**References:** [1] Jakosky, B. M., et al. (2018) *Icarus*, 315, 146–157. [2] Fox, J. L., et al. (2015) *Icarus*, 252, 366–392. [3] Krasnopolsky, V. A. (2018) *Icarus*, 321, 62–70. [4] Yung, Y. L., et al. (1988) *Icarus*, 76, 146–159. [5] Krasnopolsky, V. A. (2002) *JGR*, 107, 11. [6] Chaufray, J.-Y., et al. (2015) *Icarus*, 245, 282–294. [7] Chaufray, J.-Y., et al. (2018) *JGR*, 123, 2441–2454. [8] Chaffin, M. S., et al. (2014) *GRL*, 41, 314–320. [9] Clarke, J. T., et al. (2014) *GRL*, 41, 8013–8020. [10] Bhattacharyya, D., et al. (2015) *GRL*, 42, 8678–8685. [11] Clarke, J. T., et al. (2017) *JGR*, 122, 2336–2344. [12] Maltagliati, L., et al. (2013) *Icarus*, 223, 942–962. [13] Fedorova, A. A., et al. (2018) *Icarus*, 300, 440–457. [14] Heavens, N. G., et al. (2018) *Nat. Astron.*, 2, 126–132.